Different culture media and purification methods unveil the core proteome of Propionibacterium freudenreichii -derived extracellular vesicles

Vinícius de Rezende Rodovalho, Brenda Silva Rosa da Luz, Aurélie Nicolas, Julien Jardin, Valérie Briard-Bion, Edson Luiz Folador, Anderson Rodrigues Santos, Gwénaël Jan, Yves Le Loir, Vasco Ariston de Carvalho Azevedo, et al.

microLife, 2023, **4**, 1–15
DOI: 10.1093/femsml/uqad029
Advance access publication date: 2 June 2023
Research Article

Different culture media and purification methods unveil the core proteome of *Propionibacterium freudenreichii*-derived extracellular vesicles

Vinícius de Rezende Rodovalho[1,2,3], Brenda Silva Rosa da Luz[1,2], Aurélie Nicolas[1], Julien Jardin[1], Valérie Briard-Bion[1], Edson Luiz Folador[4], Anderson Rodrigues Santos[5], Gwénaël Jan[1], Yves Le Loir[1], Vasco Ariston de Carvalho Azevedo[2], Éric Guédon[1,*]

[1]INRAE, Institut Agro, STLO, 35042, Rennes, France
[2]Laboratory of Cellular and Molecular Genetics, Institute of Biological Sciences, Federal University of Minas Gerais, Belo Horizonte 31270-901, Brazil
[3]Laboratory of Immunoinflammation, Institute of Biology, University of Campinas (UNICAMP), Campinas 13000-000, Brazil
[4]Center of Biotechnology, Department of Biotechnology, Federal University of Paraíba, João Pessoa 58051-900, Brazil
[5]Faculty of Computer Science, Department of Computer Science, Federal University of Uberlândia, Uberlândia 38400902, Brazil
*Corresponding author. INRAE, Institut Agro, STLO, 35042, Rennes, France. E-mail: eric.guedon@inrae.fr

Abstract

Bacterial extracellular vesicles (EVs) are natural lipidic nanoparticles implicated in intercellular communication. Although EV research focused mainly on pathogens, the interest in probiotic-derived EVs is now rising. One example is *Propionibacterium freudenreichii*, which produces EVs with anti-inflammatory effects on human epithelial cells. Our previous study with *P. freudenreichii* showed that EVs purified by size exclusion chromatography (SEC) displayed variations in protein content according to bacterial growth conditions. Considering these content variations, we hypothesized that a comparative proteomic analysis of EVs recovered in different conditions would elucidate whether a representative vesicular proteome existed, possibly providing a robust proteome dataset for further analysis. Therefore, *P. freudenreichii* was grown in two culture media, and EVs were purified by sucrose density gradient ultracentrifugation (UC). Microscopic and size characterization confirmed EV purification, while shotgun proteomics unveiled that they carried a diverse set of proteins. A comparative analysis of the protein content of UC- and SEC-derived EVs, isolated from cultures either in UF (cow milk ultrafiltrate medium) or YEL (laboratory yeast extract lactate medium), showed that EVs from all these conditions shared 308 proteins. This EV core proteome was notably enriched in proteins related to immunomodulation. Moreover, it showed distinctive features, including highly interacting proteins, compositional biases for some specific amino acids, and other biochemical parameters. Overall, this work broadens the toolset for the purification of *P. freudenreichii*-derived EVs, identifies a representative vesicular proteome, and enumerates conserved features in vesicular proteins. These results hold the potential for providing candidate biomarkers of purification quality, and insights into the mechanisms of EV biogenesis and cargo sorting.

Keywords: membrane vesicles, probiotic, propionibacteria, proteomics, culture media, purification, density gradient ultracentrifugation

Introduction

Extracellular vesicles (EVs) are nano-sized membranous particles that transport biomolecules implicated in intercellular communication (Brown et al. 2015, Woith et al. 2019, Dagnelie et al. 2020, Nagakubo et al. 2020). EVs were consistently reported as an export system in species from all kingdoms of life, including bacteria (Deatherage and Cookson 2012, Woith et al. 2019, Nagakubo et al. 2020). A diverse set of functions was attributed to bacterial EVs, including quorum sensing (Mashburn and Whiteley 2005), biofilm formation (Flemming et al. 2016, Caruana and Walper 2020), competition (Li et al. 1998), nutrition (Elhenawy et al. 2014, Prados-Rosales et al. 2014), defense (Manning and Kuehn 2011, Lee et al. 2013), pathogenesis (Pathirana and Kaparakis-Liaskos 2016, Cecil et al. 2019), and probiosis (Bitto and Kaparakis-Liaskos 2017, Molina-Tijeras et al. 2019). Among beneficial bacteria, EVs with anti-inflammatory activity were reported in several species, including *Akkermansia muciniphila* (Ashrafian et al. 2019, Keshavarz Azizi Raftar et al. 2021), *Bacteroides* species (Shen et al. 2012, Mirjafari Tafti et al. 2019, Gul et al. 2022), *Escherichia coli* Nissle 1917 (Fábrega et al. 2017), *Bifidobacterium* species (López et al. 2012, Nishiyama et al. 2020), *Lactobacillus* species (Seo et al. 2018, Vargoorani et al. 2020, Caruana et al. 2021, Hao et al. 2021), and *Propionibacterium freudenreichii* (Rodovalho et al. 2020, 2021).

The functional properties of bacterial EVs, including their beneficial effects on host cells, are closely related to their cargo (Bitto and Kaparakis-Liaskos 2017, Briaud and Carroll 2020, Nagakubo et al. 2020, Cao and Lin 2021). Bacterial EVs were reported to hold a diverse set of molecules in their internal lumen, including proteins (Lee et al. 2009, Rubio et al. 2017, Bajic et al. 2020, Nishiyama et al. 2020, Bhar et al. 2021), DNA (Bitto et al. 2017, 2021a; Dell'Annunziata et al. 2021), RNA (Bitto et al. 2021a, Joshi et al. 2021, Luz et al. 2021; Pérez-Cruz et al., 2021), and metabolites (Cao et al. 2020, Kim et al. 2020, 2020ba; Sartorio et al. 2022). This vesicular content varies in response to environmental conditions, including bacterial growth media and growth phases (Bitto et al. 2021b, Briaud et al. 2021, Luz et al. 2021; Pérez-Cruz et al., 2021, Rodovalho et al. 2021, da Luz et al. 2022, Mehanny et al. 2022) and several abiotic stressors, including antibiotics, nutrient shortage,

Received 15 December 2022; **revised** 12 May 2023; **accepted** 31 May 2023

salt, and temperature (He et al. 2017, Yun et al. 2018, Godlewska et al. 2019, Lynch et al. 2019, Potter et al. 2020, Briaud et al. 2021).

Although EV cargo is modulated under diverse experimental conditions or treatments, some comparative studies reported a degree of content conservation toward changing environmental conditions (Hong et al. 2019, Monteiro et al. 2021) and bacterial strains (Hong et al. 2019, Tartaglia et al. 2020, Zwarycz et al. 2020). In the case of proteomic profiling, the conserved cargo has been referred as core proteome, meaning a set of representative proteins that occur consistently in EVs (Tartaglia et al. 2020, Zwarycz et al. 2020, Kugeratski et al. 2021). The core proteome might include proteins that are essential for EV biogenesis and cargo selection, as well as other important processes that mediate bacteria interactions with other bacteria, the host and the environment (Buschow et al. 2010, Schlatterer et al. 2018, Tartaglia et al. 2020). Therefore, the study of EV core proteomes might elucidate the roles of specific proteins, and enable a whole set of applications, including biomarker discovery (Sarshar et al. 2020, Schou et al. 2020, Urabe et al. 2020, Park et al. 2021, Useckaite et al. 2021), vaccines production (Jiang et al. 2019, Li et al. 2022), drug delivery (Yang et al. 2018, Gan et al. 2021, Zhuang et al. 2021), and immunotherapy (Gilmore et al. 2021, Holay et al. 2021, Jahromi and Fuhrmann 2021).

In our previous studies, we showed that the probiotic *P. freudenreichii* CIRM-BIA129 produces EVs with anti-inflammatory activity toward cultured human intestinal epithelial cells via NF-κB pathway modulation (Rodovalho et al. 2020) and that bacterial growth media (UF versus YEL) impact the protein composition and the anti-inflammatory activity of EVs (Rodovalho et al. 2021). Yeast extract lactate (YEL) is the gold-standard laboratory medium for propionibacteria, while ultrafiltrate (UF) medium was developed to mimic their growth conditions in Swiss-type cheeses after fermentation of the cheese curd by lactic acid bacteria (Malik et al. 1968, Cousin et al. 2012). These two media were chosen because they differentially impact the physiology of the bacterium, notably its growth parameters, the pH of the extracellular medium at the end of stationary phase, and cell viability after stress challenges (Gaucher et al. 2020b, Cousin et al. 2012). In those studies showing that the culture medium in which the bacteria are grown could be used as a lever to modulate the properties (i.e. protein composition and biological functions) of EVs, we employed size-exclusion chromatography (SEC) as a purification method. However, to better understand the relationship between the composition and functions of EVs and to optimize the growth conditions as a tool to modulate the properties of EVs, a robust characterization of their protein content is required. We thus hypothesized that a comparative proteomics study, including another EV purification method would allow a robust characterization of the EV core proteome.

In this study, we applied density gradient ultracentrifugation (UC) as an alternative method to purify EVs from the concentrated supernatants of *P. freudenreichii* CIRM-BIA129 cultures in both UF and YEL media. Then, shotgun proteomics was carried out to elucidate EVs protein content. The comparison with SEC-purified EVs from our previous studies allowed the identification of a vesicular core proteome of 308 proteins, indicating that some functional aspects were potentially conserved in *P. freudenreichii*-derived EVs obtained in four different conditions. The conserved functional categories associated with the core proteome included carbon metabolism, peptidoglycan biosynthesis, ribosome, protein export, quorum sensing, and immunomodulation. The EV core proteome also showed highly interacting proteins and compositional biases regarding specific amino acids and other biochemical parameters when compared to the whole cellular proteome. In addition to broadening the toolset for the purification of *P. freudenreichii*-derived EVs, this study also identifies a robust representative vesicular proteome for this relevant probiotic strain, providing several candidates for biomarkers of purification quality. Furthermore, it enumerates representative EV proteins and protein features, which could provide insights into mechanisms of EV biogenesis and cargo sorting for future studies.

Material and methods

Culture conditions

The strain *P. freudenreichii* CIRM-BIA129 (equivalent to the ITG P20 strain, provided by CNIEL) was supplied by the CIRM-BIA Biological Resource Center (Centre International de Ressources Microbiennes-Bactéries d'Intérêt Alimentaire, INRAE, Rennes, France). *Propionibacterium freudenreichii* was cultured either in cow milk UF (Cousin et al. 2012) or in YEL (Malik et al. 1968), both containing 100 mM sodium lactate and 5 g L^{-1} casein hydrolysate. Cultures were maintained at 30°C, without agitation, until the beginning of the stationary phase (2×10^9 bacteria mL^{-1} for UF and 3×10^9 bacteria mL^{-1} for YEL), under microaerophilic conditions.

Purification of EVs

Bacterial cultures were centrifuged (6000 x *g*, 15 min) and supernatants were filtered (0.22 mm, Nalgene top filters, Thermo Scientific) at room temperature. Cell-free supernatants were then concentrated in successive centrifugations using Amicon ultrafiltration units (100-fold, cutoff 100 kDa, 2500 x *g*). The concentrated supernatants were then submitted to a series of 3 ultracentrifugation rounds: (1) the first one to pellet EVs and discard the supernatant containing contaminant proteins (150 000 x *g*, 120 min, 4°C), (2) the second one for a higher-quality density-based separation, with the application of the resuspended pellets onto the top of a discontinuous sucrose gradient (8%–68%) (100 000 x *g*, 150 min, 4°C), and (3) a third washing step to eliminate the excess of sucrose from pooled EV-containing fractions (150 000 x *g*, 120 min, 4°C) (Tartaglia et al. 2018, 2020). The final samples were then resuspended in TBS buffer (150 mM NaCl; 50 mM Tris-Cl, pH 7.5) and used immediately or stored at 20°C.

Biophysical characterization of EVs

The size and concentration of EVs were evaluated by nanoparticle tracking analysis (NTA), using a NanoSight NS300 instrument (Malvern Panalytical, Worcestershire, UK), equipped with a sCMOS camera and a Blue488 laser. All measures were performed at 25°C, in constant flux, with a syringe pump speed of 50. For each sample, 5 videos of 60 s were recorded, under camera level 15. Other parameters were adjusted accordingly to achieve image optimization (Vestad et al. 2017, Rodovalho et al. 2020). Transmission electron microscopy (TEM) was used to evaluate the morphology, homogeneity, and integrity of EVs, as previously described (Tartaglia et al. 2018, Rodovalho et al. 2020). Briefly, glow-discharged formvar-coated copper EM grids were used for the application of a drop of EV solution and the negative staining was conducted with the application of 2% uranyl acetate to the grid. Between these steps, the grids were blotted with filter paper to remove the excess of solution. After drying, the grids were imaged using a Jeol 1400 TEM (JEOL Ltd., Tokyo, Japan) operating at 120 kV.

Mass spectrometry and protein identification

The protein cargo in EVs samples was quantified with Qubit Protein Assay Kit (Fisher Scientific, USA) and equal amounts of EV proteins were loaded onto gels and separated with 12% SDS-PAGE (Laemmli 1970). Electrophoresis was interrupted after proteins entered 5 mm of separating gel, which was fixed and silver-stained (Switzer et al. 1979). Gel pieces corresponding to each sample were then cut and subjected to in-gel trypsinolysis, peptide extraction, and nano liquid chromatography tandem mass spectrometry (nano-LC-ESI MS/MS) analysis, as previously described (Gagnaire et al. 2015, Huang et al. 2016, Gaucher et al. 2020a, Rodovalho et al. 2020). The software X! TandemPipeline was used to identify peptides from MS/MS spectra (Langella et al. 2017) and the searches were performed against the proteome of *P. freudenreichii* CIRM-BIA129 (Accession: NZ_HG975455). The database search parameters included trypsin cleavage, peptide mass tolerance set at 10 ppm for MS and 0.05 Da for MS/MS. Phosphorylation of serine and threonine residues, and methionine oxidation were set as variable modifications. The E-value threshold for peptide identification was set to 0.05 and a minimum of two peptides per replicate was required for protein identification, resulting in a false discovery rate (FDR) of < 0.15%. For each experimental condition, 3 biological replicates were investigated and the proteins were considered present if they were identified in at least 2 out of 3 replicates. The mass spectrometry proteomics data can be found at https://doi.org/10.57745/ANDSGP.

Protein sequences analysis

Propionibacterium freudenreichii CIRM-BIA129 protein sequences were retrieved from NCBI GenBank (Accession: NZ_HG975455). Ortholog-based annotation was obtained with eggNOG-mapper (Huerta-Cepas et al. 2017, 2019), including the assignment to Clusters of Orthologous Groups (COG) categories and KEGG Pathways terms. Proteomic data for UC-purified EVs were achieved within this study. Proteomic data for SEC-purified EVs were retrieved from our previous publication (Rodovalho et al. 2021). Subcellular localization and lipoprotein signals were predicted with Cello2GO (Yu et al. 2014) and PRED-LIPO (Bagos et al. 2008), respectively. Analysis and visualization with Venn diagrams and donut plots were achieved with Python libraries Pandas (McKinney 2010, The Pandas Development Team 2020), Seaborn (Waskom et al. 2017), Matplotlib_venn, and Venn; whereas bubble plots were generated with R library ggplot2 (Wickham 2016).

Functional enrichment analysis

Functional enrichment analysis was performed with g: profiler (Raudvere et al. 2019, Reimand et al. 2019), as previously described (Rodovalho et al. 2021), using KEGG terms and adopting a significance threshold (adjusted *P*-value) of 0.05. Enrichment results were represented as an enrichment network, where enriched pathways were represented as the nodes and the overlaps among them (common proteins) as edges. The enrichment network was constructed from g: profiler results and visualized with EnrichmentMap (Merico et al. 2010) and Cytoscape (Shannon et al. 2003). For the network construction, a node FDR *q*-value threshold of 0.05 was applied for functional category filtering and a threshold of 0.375 was applied for the representation of the similarity between functional categories as edges.

Prediction of protein–protein interactions

Protein-protein interactions across the whole bacterial theoretical proteome were predicted by interolog methodology, as previously described (Folador et al. 2014). Briefly, the whole bacterial proteome was aligned against the proteins in Search Tool for the Retrieval of Interacting Genes/Proteins (STRING) database (Szklarczyk et al. 2021) using Basic Local Alignment Search Tool (Altschul et al. 1990) to find reciprocal hits representing homolog proteins, with a threshold of 0.36 for the product of alignment identity and coverage. Interactions from the STRING database were filtered to a minimum quality score of 400 and were then transferred to corresponding homolog proteins in the bacterial dataset. Interactions network was visualized and analyzed with Cytoscape (Shannon et al. 2003) and Python's libraries Pandas (The Pandas Development Team 2020) and Seaborn (Waskom et al. 2017).

Machine learning and features importance

In order to evaluate which aspects of EV core proteins were distinct from other proteins, we developed a machine learning model based on protein sequences. Initially, proteins were represented as diverse types of sequence features, such as those generated with the package Biopython, including molecular weight (M.W.), isoelectric point (I.P.), aromaticity, instability, and gravy indices, secondary structure tendency for helix (ss_helix), turn (ss_turn) or sheet (ss_sheet), and the molar extinction coefficient, considering either reduced (molar_extinction_redC) or bonded cysteines (molar_extinction_oxC) (Cock et al. 2009). The package iLearn was also used to generate features corresponding to amino acid composition (AAC), di-peptide composition, grouped amino acid composition, and grouped di-peptide composition (Chen et al. 2020). The codon adaptation index (C.A.I.) was calculated with the package CAI (Lee 2018). A total of 456 sequence-related features were included in the beginning of the analysis for each protein. Proteins with features consisting of missing values were removed from analysis.

Next, sequences of bacterial proteins that were present in the EV core proteome were considered the positive class (label 1). The other proteins of the bacterial whole proteome that were absent in any of the four conditions were considered the negative class (label 0). The number of proteins in the classes was balanced with random under-sampling of the majority class using Python's package imbalanced-learn (Lemaître et al. 2017). The protein dataset was then divided into training (80%) and test (20%) datasets. The machine learning model was encapsulated in a pipeline of 3 steps: (1) univariate feature selection with f_classif (from 456 to 114 features); (2) recursive feature selection with 3-fold cross validation and Random Forest Classifier (from 114 to 102 features); and (3) an optimized Random Forest Classifier (using the best 102 features). The training dataset was fitted to the pipeline and evaluated with 5-fold cross-validation, with the construction of a receiver operating characteristic (ROC) curve and the measure of the area under the curve (AUC). The test dataset (containing unseen data by the model) was used to make predictions and comparisons with the correct (experimental) labels, using the confusion matrix representation to inspect true/false negatives/positives. These tasks were accomplished with different functionalities of Python's machine learning package Scikit-learn (Pedregosa et al. 2011). Finally, the importance of protein features for the model output was analyzed by computing the Shapley values with the package SHAP (SHapley Additive exPlanations) (Lundberg and Lee 2017, Lundberg et al. 2020).

Statistical analysis

All experiments were performed at least in triplicate and the numerical results are expressed as mean ± standard deviation, unless specified otherwise. For significance evaluation, one-way ANOVA was performed with Tukey's multiple-comparison test.

Results

EVs concentration and size distribution vary according to purification methods and culture media

In this study, we evaluated the properties of UC-purified *P. freudenreichii*-derived EVs. The samples obtained after a series of UC steps were analyzed by TEM and NTA, confirming the purification of EVs with typical spherical shape (Fig. 1A) and nanometric size distribution (Fig. 1B). The properties of UC-purified EVs were then compared with those of SEC-purified EVs, reported in our previous study (Rodovalho et al. 2021). Therefore, we compared four conditions: UF-derived EVs purified by UC (UC_UF), YEL-derived EVs purified by UC (UC_YEL), UF-derived EVs purified by SEC (SEC_UF), and YEL-derived EVs purified by SEC (SEC_YEL). EVs obtained by both purification methods (UC and SEC) and from both culture media (UF and YEL) presented similar monodispersed size distributions, although with different concentrations and modal diameters (Fig. 1B). Although all EV groups presented modal diameters in the range 75–90 nm, EV modal diameter was significantly higher for SEC_YEL EVs, notably when compared to the UC_YEL group (Fig. 1C). The yield (the ratio between the amount of recovered EVs and bacterial cells count at sampling time) was lower for UC_UF EVs, thus all other groups values were normalized in relation to this group. The relative yield was 8.3 times higher for SEC_UF and 2.5 times higher for SEC_YEL, and not significatively different for UC_YEL (Fig. 1D). This comparison showed that the purification methods can impact the yield but also the type of recovered EVs.

EVs protein content varies according to purification methods and culture media

In order to see whether the EV purification method can also impact their composition, UC-purified EVs were then biochemically analyzed, regarding their protein content. A total of 598 proteins were identified in UC-purified EVs, 560 of which were shared among UF- and YEL-derived EVs. The resulting dataset was then compared with the one previously obtained from SEC-purified EVs and available at https://doi.org/10.15454/Q6PPXY (Rodovalho et al. 2021). Comparative proteomics of UC- and SEC-purified EVs showed that although some proteins were exclusive to one or more conditions, 308 proteins were identified in all four conditions, comprising the EV core proteome (Fig. 2A). Likewise, 302 proteins were identified in more than one condition, but not in all conditions, comprising the accessory proteome; and 42 proteins were restricted to one of the conditions, comprising the exclusive proteome (Fig. 2B). A greater difference of protein content was associated to EVs purification method, since a great number of proteins was exclusively found in EVs purified by UC ($n = 261$) and by SEC ($n = 54$). A smaller number of proteins was exclusive to EVs recovered from specific culture media: SEC_UF_only ($n = 7$), SEC_YEL_only ($n = 1$), UC_UF_only ($n = 32$), and UC_YEL_only ($n = 2$) (Fig. 2A). Altogether, the purification methods selected different subpopulations of EVs that differ by their protein content.

Major differences in the characteristics of EV proteins are associated to the purification method

As the comparative proteomics analysis showed that EVs purification method had a dramatic impact on the protein content, particularly regarding EVs_UC_only ($n = 261$) and EVs_SEC_only ($n = 54$) groups, we analyzed the functional and subcellular localization characteristics of those proteins that were exclusive to each purification method. Regarding subcellular localization, most proteins were predicted to be cytoplasmic, although some of them were predicted to be extracellular in UC_only group ($n = 10$), or membrane proteins in UC-only ($n = 26$) and SEC-only ($n = 11$) groups (Fig. 3A). Lipoprotein signals were identified in UC_only group ($n = 5$), although secretory and transmembrane signals were also identified in UC_only and SEC_only groups (Fig. 3B). Regarding COG categories, these groups contained proteins that were assigned to multiple categories, with UC_only proteins being well distributed among most of these categories (Fig. 3C). Therefore, the proteins associated to each group showed specific features, although UC_only was a larger and more diverse group.

The core proteome of *P. Freudenreichii*-derived EVs is mainly related to metabolic functions

In order to understand what are the conserved features of EVs protein content, we further analyzed their core proteome. The assignment of COG categories showed that almost half of the core proteins were related to metabolic processes, although some were related to cellular processes, like cell envelope biogenesis; and information storage and processing, including replication, transcription, and translation (Fig. 4A). Regarding subcellular localization, almost three quarters of these proteins were predicted to be cytoplasmic (70.5%), although membrane (17.5%) and extracellular (12%) proteins were also identified (Fig. 4B). Lipoprotein signals were present in only 8.1% of the core proteins, whereas transmembrane (12.7%) and secretion (7.5%) signals were also identified (Fig. 4C). Functional enrichment analysis with KEGG terms demonstrated these proteins were mainly related to central carbon metabolism, but also implicated in peptidoglycan biosynthesis, ribosome, protein export, and quorum sensing (Fig. 4D).

Furthermore, some of the proteins identified in the EV core proteome were previously identified as immunomodulatory in studies with strains of *P. freudenreichii* (Table 1).

Finally, some of the proteins within the EV core proteome were predicted to be membrane-localized (Cello2GO) and contain transmembrane signals (LIPO-PRED) (Table 2). These proteins could be further studied as potential markers of purification quality, since they are surface-accessible and consistently present in EVs.

The predicted bacterial interactome shows that EVs proteins tend to interact more than other proteins

As the EV core proteome provided a robust set of proteins consistently loaded into EVs, we used this dataset to investigate potential protein interactions as a relevant feature to determine protein sorting into EVs. Therefore, we used a homology-based method to predict protein–protein interactions between members of the whole bacterial proteome. These predictions resulted in a network with 2092 nodes, 86 317 edges, 7 connected components, and a network diameter of 8. Among the interacting proteins, those belonging to the EV core proteome showed generally central positions in the network (Fig. 5A). The number of interactions per protein, i.e. their degree, showed a typical power-law distribution, as expected for biological networks (Fig. 5B). When analyzed over different proteins groups, the degree distribution showed great variability, but the median degree was higher for those proteins belonging to EVs (EVs_core, EVs_SEC_only, EVs_UC_only, and EVs_other) than for those not belonging to EVs (Not EVs) (Fig. 5C). Therefore, these results show that higher degree centrality could

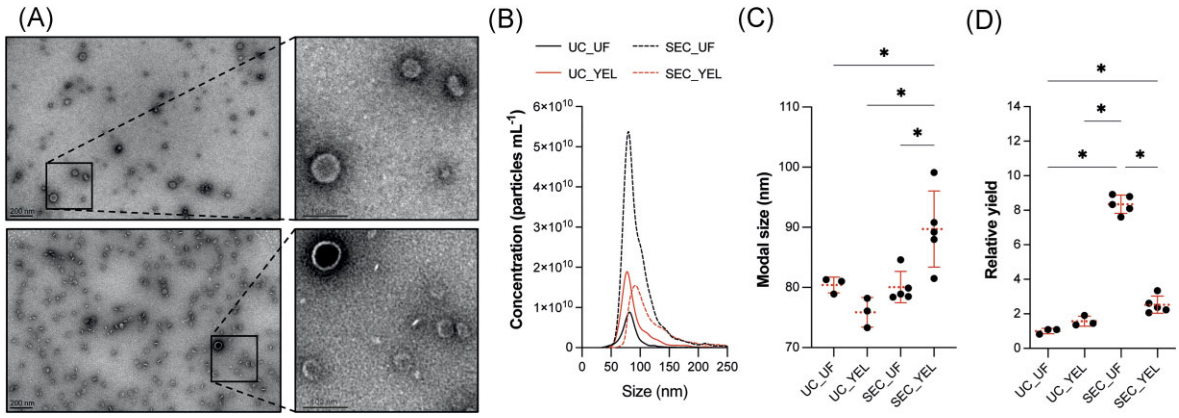

Figure 1. Biophysical characteristics of *P. freudenreichii*-derived EVs. **(A)** Transmission electron microscopy of EVs purified from YEL (upper panel) and UF (lower panel) medium with UC method at two magnifications. **(B)** Size distribution of UF- and YEL-derived EVs purified with UC and SEC methods. Shown are curves of a representative biological triplicate. **(C)** Modal diameter of UF- and YEL-derived EVs purified with UC and SEC methods. **(D)** Ratio between the amount of recovered EVs and bacterial cells (CFU counting) at sampling time, normalized relative to UF-derived EVs. Each data point corresponds to a biological replicate, dashed line represents mean and solid line indicates standard deviation. Data from SEC-purified EVs were extracted from our previous study for comparison (Rodovalho et al. 2021). Ordinary one-way ANOVA followed by Tukey's multiple-comparison test was performed. Only comparisons with *P* value less than or equal to 0.05 (indicated by ∗) were represented.

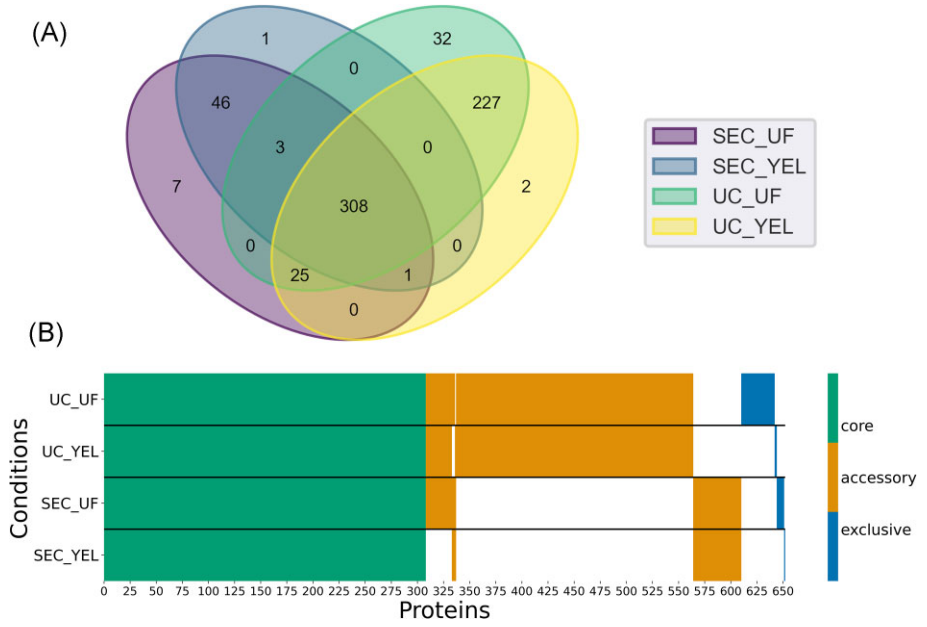

Figure 2. Proteins distribution according to condition of EV obtention. **(A)** Venn diagram presenting the number of proteins per condition and intersections. **(B)** Heatmap representing the presence (colored) or absence (white) of all the analyzed proteins in each condition of EV obtention. Core: core proteome, proteins present in all four conditions. Accessory: accessory proteome, proteins present in 2 or 3 conditions. Exclusive: exclusive proteome, proteins present in only one condition. (A)–(B) UC_UF: UF-derived EVs purified by UC. UC_YEL: YEL-derived EVs purified by UC. SEC_UF: UF-derived EVs purified by SEC. SEC_YEL: YEL-derived EVs purified by SEC. Data from UC-purified EVS were achieved in this study and data from SEC-purified EVs were recovered from our previous study (Rodovalho et al. 2021).

Table 1. Proteins from the EV core proteome that were identified as immunomodulatory in other studies with strains of *P. freudenreichii*.

Protein	GI	Description	COG	Localization	Lipoprotein signal prediction
Eno1	659917660	Enolase 1	G	Cytoplasmic	Other
Acn	659918109	Aconitase	C	Cytoplasmic	Other
GroL2	659917458	60 kDa chaperonin 2	O	Cytoplasmic	Other
SlpE	659917805	Surface layer protein E	O	Extracellular	Sec
SlpB	659918413	Surface layer protein B	O	Extracellular	Sec
PFCIRM129_10785	659917415	Hypothetical protein	?	Membrane	Lipo

Legend: Sec: secretion signal peptide, Lipo: lipoprotein signal peptide, TM: transmembrane, Other: no signals found, ?: unknown. References: Deutsch et al. (2017), Do Carmo et al. (2017, 2019).

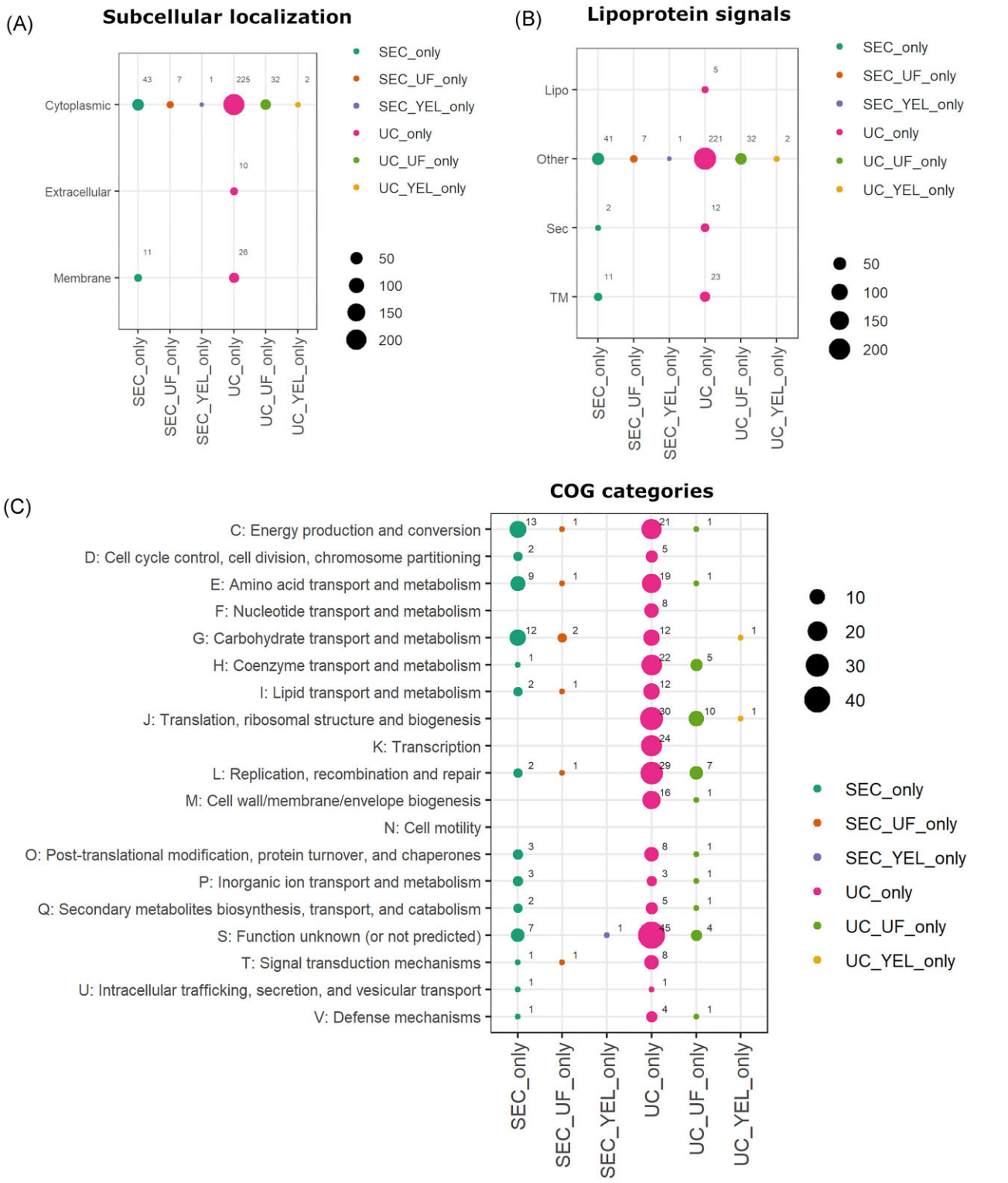

Figure 3. Comparison of vesicular proteomes' characteristics according to condition of EV obtention. **(A)** Proteins subcellular localization, as predicted by Cello2GO. **(B)** Lipoproteins signals prediction by LIPO-PRED. Sec: secretion signal peptide. Lipo: lipoprotein signal peptide. TM: transmembrane. Other: no signals found. **(C)** COG categories assignment. SEC_only: proteins retrieved in SEC-purifed EVs, but not in UC-purified EVs. SEC_UF_only: proteins exclusive to SEC-purified UF-derived EVs. SEC_YEL_only: proteins exclusive to SEC-purified YEL-derived EVs. UC_only: proteins retrieved in UC-purifed EVs, but not in SEC-purified EVs. UC_UF_only: proteins exclusive to UC-purified UF-derived EVs. UC_YEL_only: proteins exclusive to UC-purified YEL-derived EVs.

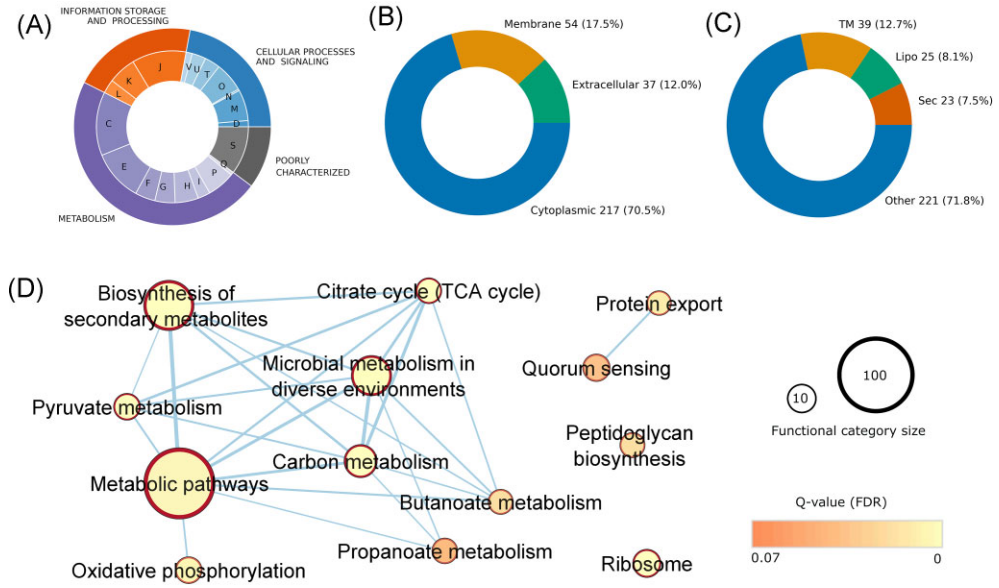

Figure 4. Functional and spatial features of the EV core proteome. **(A)** Distribution of COG categories. **(B)** Protein subcellular localizations, as predicted by Cello2GO. **(C)** Lipoproteins prediction by LIPO-PRED. Sec: secretion signal peptide. Lipo: lipoprotein signal peptide. TM: transmembrane. Other: no signals found. **(D)** Enrichment map obtained from functional enrichment analysis of KEGG Pathways terms. Node sizes are proportional to functional category set size. Edges indicate shared proteins among the linked sets. Color is related to statistical significance (Q-value). For COG categories legend, see Fig. 3.

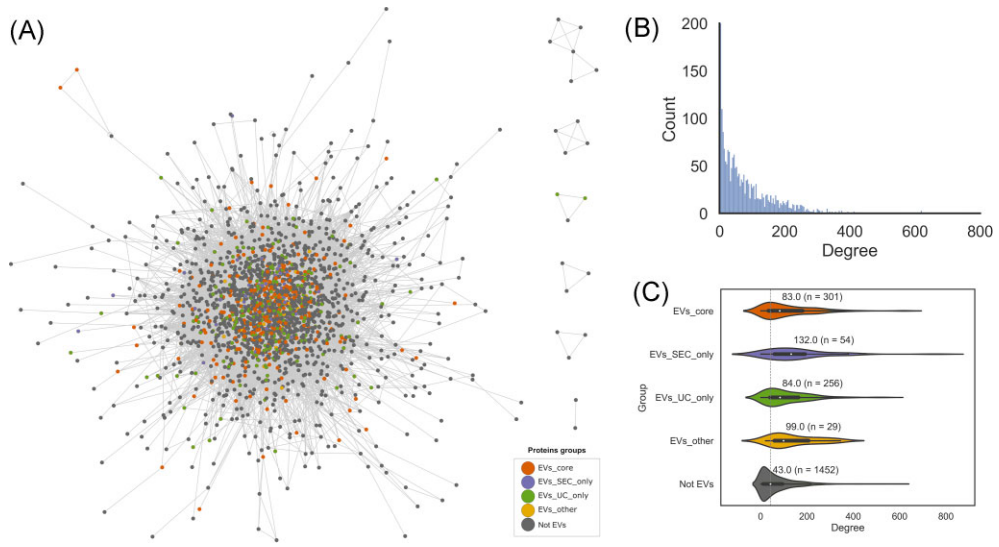

Figure 5. Predicted interactions for the proteins belonging or not to EVs. **(A)** Network of interacting bacterial proteins, where circles correspond to proteins and grey lines represent the interactions. **(B)** Degree distribution for all proteins, represented as an histogram of frequencies of interactions per protein. **(C)** Violin plot representing the degree distribution according to protein groups. Median degree and sample size are also textually assigned to each group. EVs_core: group of proteins belonging to the EV core proteome, EVs_SEC_only: proteins belonging exclusively to SEC-purified EVs, EVs_UC_only: proteins belonging exclusively to UC-purified EVs, EVs_other: proteins belonging to EVs obtained in other conditions, and Not EVs: proteins not found in EVs in any condition.

be an important feature of the EV core proteome, with potential implications on protein-mediated cargo sorting.

A random forest model unveils important sequence features of the EV core proteome

Finally, we built a random forest model comparing proteins that were present or absent in the EV core proteome, in the aim to evaluate relevant sequences features, including amino acid composition and other properties. The total dataset was balanced, to avoid biases; and divided into different datasets to avoid data leakage during the distinct phases of model development (training and test). The ROC curve resulting from the 5-fold cross-validation of training phase showed an AUC of 0.83 ± 0.02, indicating a reasonable performance (Fig. 6A). The confusion matrix for model predictions with the test dataset showed a good proportion of correctly labeled predictions in the main diagonal (Fig. 6B), with AUC of 0.8, weighted average f1-score of 0.8, and MCC of 0.6 for the test dataset (Table 3). The summary plot of features importance and features effects unveiled which sequences features were the most relevant for the model output, including the composition of cer-

Table 2. Proteins from the EV core proteome that are potential markers of purification quality.

Protein	GI	Description	COG category	Subcellular localization	Lipoprotein signal
CbiM	659918653	Cobalt transport protein CbiM	P	Membrane	TM
CbiN	659918654	Cobalt transport protein CbiN	P	Membrane	TM
CodB	659916960	Permease for cytosine/purines, uracil, thiamine,allantoin	F	Membrane	TM
CstA	659917091	Carbon starvation protein	T	Membrane	TM
CycA1	659916913	D-serine/D-alanine/glycine transporter	E	Membrane	TM
Dac	659916853	carboxypeptidase (serine-type D-Ala-D-Ala carboxypeptidase) (D-alanyl-D-alanine-carboxypeptidase)	M	Membrane	TM
FtsW2	659916822	Cell division protein	D	Membrane	TM
GlpT	659917186	Glycerol-3-phosphate transporter	G	Membrane	TM
IolT3	659917518	iolT3 (myo-inositol transporter iolT3)	EGP	Membrane	TM
LepB	659919139	Signal peptidase I	U	Membrane	TM
MetQ	659916945	ABC-type transport systems, periplasmic component	P	Membrane	TM
PFCIRM129_00555	659917047	Sugar transporter	EGP	Membrane	TM
PFCIRM129_02060	659916840	Hypothetical protein	S	Membrane	TM
PFCIRM129_02885	659918305	Hypothetical secreted and membrane protein	T	Membrane	TM
PFCIRM129_05605	659917786	Hypothetical protein	NU	Membrane	TM
PFCIRM129_07390	659918769	Hypothetical protein	S	Membrane	TM
PntB	659916763	NADH dehydrogenase	C	Membrane	TM
SdhC1	659918268	Succinate dehydrogenase subunit C	C	Membrane	TM
SdhC2	659919143	Succinate dehydrogenase cytochrome B-558 subunit	S	Membrane	TM
SecD	659918024	Protein-export membrane protein secD	U	Membrane	TM
SecF	659918023	Protein-export membrane protein secF	U	Membrane	TM
SlgT	659918370	Sodium/glucose cotransporter (Na(+)/glucose symporter) 2.A.21.3.2	E	Membrane	TM
YdfJ	659917797	Drug exporters of the RND superfamily	P	Membrane	TM
YihN	659917150	Membrane protein, Transporter, MFS superfamily	G	Membrane	TM

Table 3. Performance metrics in training and test phases of the classification model development.

Performance metrics	Training dataset	
($n = 316$)	Test dataset	
($n = 80$)		
AUC	0.83 ± 0.02 (5-fold)	0.80
MCC	n.a.	0.60
Precision (weighted avg)	n.a.	0.80
Recall (weighted avg)	n.a.	0.80
f1-score (weighted avg)	n.a.	0.80

Legend: n.a.: not applicable, AUC: area under the ROC curve; MCC: Matthews correlation coefficient; weighted avg: class-weighted average.

tain amino acids, such as lysine (K) and asparagine (N), as well as other sequence-related properties, such as C.A.I. and molecular weight (Fig. 6C). The summary plot also shows that higher values of some features (e.g. lysine, asparagine and serine content, non-polar amino acid duos, C.A.I., and molecular weight) had a positive impact on model output; whereas for other features (e.g. PD dipeptides), lower values had a positive impact on model output (Fig. 6C).

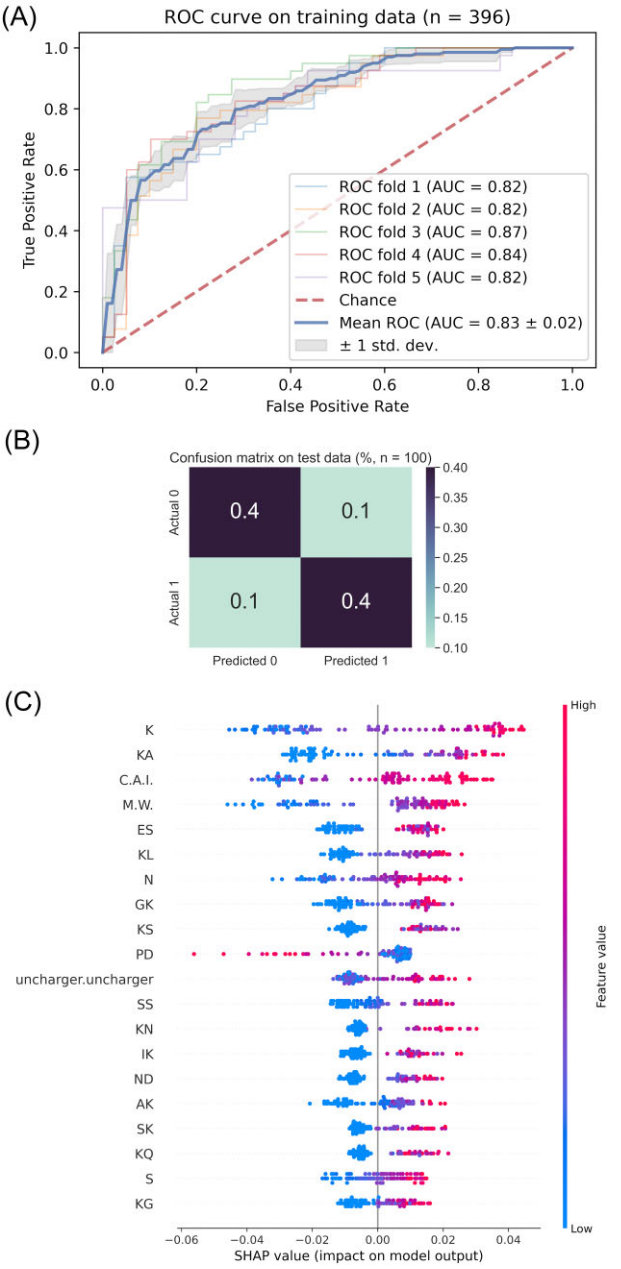

Figure 6. Model performance and features importance of the protein sequences belonging to the EV core proteome (1) or not (0). **(A)** Receiver operating characteristic (ROC) curve for the 5-fold cross-validation of the model with the training dataset ($n = 396$). **(B)** Confusion matrix for the model on the test dataset ($n = 100$). The matrix rows correspond to class predictions and the columns correspond to the actual classes. The matrix shows the percentage of proteins that are predicted to be of one class and are either correctly labeled or mislabeled by the model. Class 1 corresponds to proteins that are present in the EV core proteome and class 0 corresponds to proteins that are absent. **(C)** Summary plot of features importance and features effects, showing different features ordered according to decreasing importance (Y-axis) and their impact on model output as Shapley values (X-axis). Colors represent feature values (from low to high). C.A.I.: codon adaptation index; M.W.: molecular weight; uncharger.uncharger: duos of uncharged amino acids. All other letters represent one-letter identification of amino acids.

Discussion

We previously purified *P. freudenreichii*-derived EVs from cultures in UF and YEL using SEC (Rodovalho et al. 2020, 2021). In this study, we report their purification using another method (UC), both from cultures, in UF and YEL media. UC-based purification uses high-speed centrifugation to separate EVs and contaminants by differential sedimentation, whereas SEC is based on the differential elution of EVs and contaminants through a porous polymeric matrix with specific molecular weight cut-off (Klimentová and Stulík 2015, Monguió-Tortajada et al. 2019, McNamara and Dittmer 2020). SEC is an approach of rising relevance, scalable and fast, that preserves EV structure and activity, although it has limitations in sample volume and co-purification of particles of similar sizes, such as viruses (Nordin et al. 2015, Benedikter et al. 2017, Mol et al. 2017, Monguió-Tortajada et al. 2019, McNamara and Dittmer 2020). At the same time, UC is time-consuming and operator-dependent, with risks of inducing EV aggregation and damaging, although it results in reliable high-purity EV samples, being the most used approach for bacterial EV recovery (Mol et al. 2017, Monguió-Tortajada et al. 2019). Each method presents advantages and drawbacks, and its application should account for the complex tradeoff between higher EV yields and less amounts of contaminants (Dauros Singorenko et al. 2017). Anyhow, as confirmed by TEM images and NTA measurements, it was possible to recover EVs of typical nanometric sizes and spherical cup-shaped morphology using UC-based purification, similarly to what we previously described for SEC-based purification.

Regarding the biophysical properties of UC-purified EVs, there was no difference between UC_UF and UC_YEL EVs in terms of modal diameter and only a subtle difference regarding EV abundance relative to bacterial cells, yet not significant. Contrastingly, our study with SEC-purified EVs had shown that SEC_YEL EVs were larger and less abundant than SEC_UF EVs (Rodovalho et al. 2021). The observed disparities in abundance levels between the two purification methods could potentially be attributed to the varying effectiveness of each method in retrieving EVs. By eliminating contaminant particles, which could include bioactive proteins, nucleic acids, and metabolites, both methods strive to generate a predominantly EV-based preparation. The differences in sizes could be due to the purification of different EVs subpopulations by each method, with distinct biophysical and biochemical properties (Dauros Singorenko et al. 2017, Gho and Lee 2017). Another possibility is that the purification methodologies could trigger physical deformations, such as the aggregation reported for UC-based methods (Mol et al. 2017, Monguió-Tortajada et al. 2019). Although the purification methods impacted on EVs biophysical properties, there was no abnormal difference and EVs with typical biophysical properties were retrieved in all the four analyzed conditions.

In line with what we previously verified for SEC-purified EVs, bacteria growth conditions also modulated the protein content of UC-purified EVs. There were 35 proteins exclusive to UC_UF EVs and 3 proteins exclusive to UC_YEL EVs, although the majority of 560 proteins were common to both conditions of culture. In our previous study with SEC-purified EVs, 32 proteins were exclusive to SEC_UF EVs and 1 protein was exclusive to SEC_YEL EVs, with 358 proteins common to both conditions of culture (Rodovalho et al. 2021). Therefore, although a similar distribution was verified among exclusive and common proteins, 50% more proteins were identified in UC-purified EVs, in comparison to SEC-purified EVs. Again, the reason could be the purification of distinct subpopulations by the two methods, which would result in protein

content variations (Dauros Singorenko et al. 2017, Gho and Lee 2017). Another possibility is that UC-based purification could be less efficient for *P. freudenreichii*-derived EVs, thus resulting in the co-purification of more contaminant proteins, when compared to SEC-based purification (Mol et al. 2017). Further studies with the optimization of parameters such as molecular weight cutoff for SEC and density gradient composition for UC, as well as single EV characterization, could elucidate the occurrence of EVs subpopulations and critically evaluate the purity of the samples (Dauros Singorenko et al. 2017, Gho and Lee 2017, Mol et al. 2017).

Nonetheless, 308 proteins were consistently identified in EVs from both purification methods and growth conditions, indicating that a particular set of proteins—the EV core proteome—is invariably present in *P. freudenreichii*-derived EVs, considering the four analyzed conditions. This is a robust and representative set of proteins to be used in further analysis of *P. freudenreichii* EV proteome, since it is less susceptible to purification and growth biases. This core proteome comprises extracellular and membrane-associated proteins, although the main composition correspond to cytoplasmic proteins (more than 70%), which is consistent with several proteomic analysis of EVs derived from Gram-positive bacteria (Lee et al. 2009, Brown et al. 2015, Kim et al. 2015, Briaud and Carroll 2020).

Regarding the functional aspects of the core proteome, some of the identified proteins were previously associated to immunomodulation in *P. freudenreichii*. Those included Enolase 1 (Eno1), Aconitase (Acn), 60 kDa chaperonin 2 (GroL2), Surface-layer proteins B (SlpB) and E (SlpE), and a hypothetical protein (PFCIRM129_10785) (Deutsch et al. 2017; do Carmo et al. 2019). Importantly, we demonstrated that SlpB was partly involved in the immunomodulatory activity of SEC-purified EVs (Rodovalho et al. 2020), in accordance with its key role in the interaction with the host that has been demonstrated for *P. freudenreichii* bacterial cells as well (do Carmo et al. 2017, 2019). Whether UC-purified EVs also exert an immunomodulatory activity should be further investigated, but the identification of these proteins in the core proteome is a promising indicator.

Moreover, proteins with functions related to peptidoglycan metabolism were identified in the core proteome, including the transferases MurG (659917354, CDP49364.1) and MurA (659917556, CDP49091.1); endopeptidases such as the secreted cell-wall peptidase of the NlpC/P60 family (659918631, CDP48034.1) and the hypothetical proteins PFCIRM129_03060 (659918230, CDP48413.1) and PFCIRM129_10650 (659917426, CDP49227.1); the transpeptidases cell division protein FtsI (659917360, CDP49370.1) and penicillin-binding protein A (659916821, CDP49790.1); and a carboxypeptidase (659916853, CDP49718.1). These identifications reinforce a hypothesis for EVs biogenesis in Gram-positive bacteria, that involves cell-wall remodeling via enzymatic action (Toyofuku et al. 2017, Briaud and Carroll 2020). The core proteome was also enriched in central metabolism enzymes and ribosomes components, which could have a role as public goods for the bacterial population, serving as metabolic and structural complements for individual bacterial cells (Rakoff-Nahoum et al. 2014, Valguarnera et al. 2018). In other environments, such as dairy matrices with multiple strains or the human gastrointestinal tract, the export of such proteins might exert a crucial role in adaptation and interspecies interactions (Rakoff-Nahoum et al. 2014, Liu et al. 2018). That is also true for other enriched terms in the core proteome, such as protein export and quorum sensing, which also mediate bacterial interactions and comprise transporter and signal recognition proteins with important roles in adaptation.

Our analysis of the EV core proteome also indicated that it contains some highly interacting proteins, such as Pyruvate-flavodoxin oxidoreductases (NifJ1, NifJ2), Inosine-5-monophosphate dehydrogenases (GuaB1, GuaB3), Recombinase A (RecA), Translation initiation factor IF-2 (InfB), and DNA-directed RNA polymerase subunit beta (RpoB), which could function as hubs in the bacterial protein interactome. Although these proteins have evident roles in metabolism and information processing, some of them have homologs listed as moonlighting proteins at MoonProt database (Chen et al. 2021). This suggests that they may play alternative roles, such as regulatory roles, binding to mucins, macromolecular structures, and human cells (Granato et al. 2004, Kesimer et al. 2009). Moreover, they could benefit from their interaction capability to play other roles in the vesicular context, related to the recruitment and selection of protein content into EVs. Although their presence in the core proteome and interactome patterns are good evidences, this hypothesis should be addressed with further investigation in the future.

Furthermore, our machine learning model showed that some sequences features tend to be more common in EV core-associated proteins than in other proteins of the bacterial predicted proteome. These features include higher lysine (K), asparagine (N) and serine (S) content, higher C.A.I., and higher molecular weight (M.W.), among others. The specific favored amino acid composition may be indicative of protein modifications that would direct proteins into EVs, such as lysine acetylation, asparagine N-glycosylation, and serine O-glycosylation (Macek et al. 2019). However, instead of (or in addition to) protein modification, these differential patterns of AAC could be related to physicochemical properties, including charge, hydrogen bonding, and molecular weight, which could also direct protein pre-accumulation for loading into EVs (Xu et al. 2013). Additionally, higher values of C.A.I. were also verified in proteins present in EVs, which could indicate that highly expressed proteins are preferentially loaded into EVs, since C.A.I. is considered a proxy of protein expression (Sharp and Li 1987, dos Reis 2003). Our results are in accordance with our previous report regarding *Staphylococcus aureus*-derived EVs, which also included proteins with higher C.A.I. values and also showed amino acids compositional biases, including higher lysine content (Tartaglia et al. 2020). Although our model showed reasonable performance, with AUC of 0.83 and 0.80 for cross-validation training and testing, respectively; there is room for improvement. The encoding with other types of features, including structural and evolutionary information, as well as data from other omics sciences, could significantly improve the performance of future versions of this model, together with the implementation of other algorithmic strategies. Moreover, it is important to apply similar schemes to other species of bacteria to investigate if these findings are species-specific or if they generalize to other Gram-positive bacteria.

Overall, we demonstrated that the UC purification method, applied to cultures of *P. freudenreichii* in UF and YEL media, also yielded EVs of typical shape and size, similar to SEC-purified EVs. Moreover, UC-purified EVs presented biophysical properties that were less variable according to growth conditions than those of SEC-purified EVs. Nonetheless, the protein content varied according to growth conditions in UC-purified EVs, and it was more extensive than that of SEC-purified EVs. Finally, the combination of the proteomic dataset from the four studied conditions allowed the identification of 308 invariably occurring proteins. This core proteome comprises a more representative dataset of the proteins from *P. freudenreichii*-derived EVs and probably relates to their es-

sential roles, including immunomodulation, carbon metabolism, peptidoglycan biosynthesis, ribosome, protein export, and quorum sensing. This is consistent with the recognized role of EVs in intercellular communication, in nutrition, and in probiosis. This core proteome also showed relatively distinctive features, including the presence of highly interacting proteins, specific amino acids composition, molecular weight, and C.A.I.. Further analysis of this core proteome is promising for the elucidation of key aspects of *P. freudenreichii*-derived EVs, including mechanisms of biogenesis, cargo sorting and interactions with the host.

Author contributions

Vinícius de Rezende Rodovalho, Gwénaël Jan, Yves Le Loir, Vasco Ariston de Carvalho Azevedo, and Éric Guédon conceived and designed the experiments. Vinícius de Rezende Rodovalho, Valérie Briard-Bion, Julien Jardin, and Brenda Silva Rosa da Luz performed the experiments. Vinícius de Rezende Rodovalho, Edson Luiz Folador, Anderson Rodrigues dos Santos, Aurélie Nicolas, Julien Jardin, and Éric Guédon analyzed the data. Aurélie Nicolas, Julien Jardin, Valérie Briard-Bion, Edson Luiz Folador, Anderson Rodrigues dos Santos, Gwénaël Jan, and Éric Guédon gave practical suggestions to perform experiments. Vasco Ariston de Carvalho Azevedo, Yves Le Loir, and Éric Guédon contributed to funding acquisition. Vinícius de Rezende Rodovalho and Éric Guédon wrote the original draft. All authors contributed to data interpretation, drafting the manuscript, critically revising the manuscript and approved its final version.

Acknowledgments

This work benefited from the facilities and expertise of the MRic-TEM platform (https://microscopie.univ-rennes1.fr). The authors are grateful to Agnès Burel (Univ. Rennes, BIOSIT—UMS 3480, US_S 018, Rennes, France) for sessions with the microscope. The authors thank the CNIEL (Centre National Interprofessionnel de l'Economie Laitière) for providing the ITG P20 strain (alias CIRM-BIA129) of *Propionibacterium freudenreichii*.

Supplementary data

Supplementary data is available at FEMSML online.

Conflict of interest statement. The authors declare no conflict of interest.

Funding

This work has received a financial support from INRAE (Rennes, France) and Institut Agro (Rennes, France). Vinícius de Rezende Rodovalho and Brenda Silva Rosa da Luz were supported by the International Cooperation Program CAPES/COFECUBat the Federal University of Minas Gerais funded by CAPES—the Brazilian Federal Agency for the Support and Evaluation of Graduate Education of the Brazilian Ministry of Education (number 99999.000058/2017-03 and 88887.179897/2018-00, respectively).

References

Altschul SF, Gish W, Miller W *et al.* Basic local alignment search tool. *J Mol Biol* 1990;**215**:403–10. https://doi.org/10.1016/S0022-2836(05)80360-2.

Ashrafian F, Shahriary A, Behrouzi A *et al.* Akkermansia muciniphila-derived extracellular vesicles as a mucosal delivery vector for amelioration of obesity in mice. *Front Microbiol* 2019;**10**:2155. https://doi.org/10.3389/fmicb.2019.02155.

Bagos PG, Tsirigos KD, Liakopoulos TD *et al.* Prediction of lipoprotein signal peptides in Gram-positive bacteria with a Hidden Markov Model. *J Proteome Res* 2008;**7**:5082–93. https://doi.org/10.1021/pr800162c.

Bajic SS, Cañas M-A, Tolinacki M *et al.* Proteomic profile of extracellular vesicles released by Lactiplantibacillus plantarum BGAN8 and their internalization by non-polarized HT29 cell line. *Sci Rep* 2020;**10**:21829. https://doi.org/10.1038/s41598-020-78920-z.

Benedikter BJ, Bouwman FG, Vajen T *et al.* Ultrafiltration combined with size exclusion chromatography efficiently isolates extracellular vesicles from cell culture media for compositional and functional studies. *Sci Rep* 2017;**7**:1–13. https://doi.org/10.1038/s41598-017-15717-7.

Bhar S, Edelmann MJ, Jones MK. Characterization and proteomic analysis of outer membrane vesicles from a commensal microbe, Enterobacter cloacae. *J Proteomics* 2021;**231**:103994. https://doi.org/10.1016/j.jprot.2020.103994.

Bitto NJ, Chapman R, Pidot S *et al.* Bacterial membrane vesicles transport their DNA cargo into host cells. *Sci Rep* 2017;**7**:1–11. https://doi.org/10.1038/s41598-017-07288-4.

Bitto NJ, Cheng L, Johnston EL *et al.* Staphylococcus aureus membrane vesicles contain immunostimulatory DNA, RNA and peptidoglycan that activate innate immune receptors and induce autophagy. *J Extracell Vesicle* 2021;**10**. https://doi.org/10.1002/jev2.12080.

Bitto NJ, Kaparakis-Liaskos M. The therapeutic benefit of bacterial membrane vesicles. *Int J Mol Sci* 2017;**18**:1–15. https://doi.org/10.3390/ijms18061287.

Bitto NJ, Zavan L, Johnston EL *et al.* Considerations for the analysis of bacterial membrane vesicles: methods of vesicle production and quantification can influence biological and experimental outcomes. *Microbiol Spectr* 2021;**9**:1–15. https://doi.org/10.1128/Spectrum.01273-21.

Briaud P, Carroll RK. Extracellular vesicle biogenesis and functions in Gram-positive bacteria. *Infect Immun* 2020;**88**:1–37. https://doi.org/10.1128/IAI.00433-20.

Briaud P, Frey A, Marino EC *et al.* Temperature influences the composition and cytotoxicity of extracellular vesicles in *Staphylococcus* aureus. *mSphere* 2021;**6**:1–16. https://doi.org/10.1128/mSphere.00676-21.

Brown L, Wolf JM, Prados-Rosales R *et al.* Through the wall: extracellular vesicles in Gram-positive bacteria, mycobacteria and fungi. *Nat Rev Microbiol* 2015;**13**:620–30. https://doi.org/10.1038/nrmicro3480.

Buschow SI, Balkom BWM, Aalberts M *et al.* MHC class II-associated proteins in B-cell exosomes and potential functional implications for exosome biogenesis. *Immunol Cell Biol* 2010;**88**:851–6. https://doi.org/10.1038/icb.2010.64.

Cao Y, Lin H. Characterization and function of membrane vesicles in Gram-positive bacteria. *Appl Microbiol Biotechnol* 2021;**105**:1795–801. https://doi.org/10.1007/s00253-021-11140-1.

Cao Y, Zhou Y, Chen D *et al.* Proteomic and metabolic characterization of membrane vesicles derived from *Streptococcus* mutans at different pH values. *Appl Microbiol Biotechnol* 2020;**104**:9733–48. https://doi.org/10.1007/s00253-020-10563-6.

Caruana J, Dean S, Walper S. Isolation and characterization of membrane vesicles from *Lactobacillus* species. *BIO-PROTOCOL* 2021;**11**:1–11. https://doi.org/10.21769/BioProtoc.4145.

Caruana JC, Walper SA. Bacterial membrane vesicles as mediators of microbe–microbe and microbe–host community interactions. *Front Microbiol* 2020;**11**:432. https://doi.org/10.3389/fmicb.2020.00432.

Cecil JD, Sirisaengtaksin N, O'Brien-Simpson NM *et al.* Outer membrane vesicle-host cell interactions. *Microbiol Spectr* 2019;**7**:201–14. https://doi.org/10.1128/microbiolspec.psib-0001-2018.

Chen C, Liu H, Zabad S *et al.* MoonProt 3.0: an update of the moonlighting proteins database. *Nucleic Acids Res* 2021;**49**:D368–72. https://doi.org/10.1093/nar/gkaa1101.

Chen Z, Zhao P, Li F *et al.* ILearn: an integrated platform and meta-learner for feature engineering, machine-learning analysis and modeling of DNA, RNA and protein sequence data. *Brief Bioinform* 2020;**21**:1047–57. https://doi.org/10.1093/bib/bbz041.

Cock PJA, Antao T, Chang JT *et al.* Biopython: freely available Python tools for computational molecular biology and bioinformatics. *Bioinformatics* 2009;**25**:1422–3. https://doi.org/10.1093/bioinformatics/btp163.

Cousin FJ, Louesdon S, Maillard MB *et al.* The first dairy product exclusively fermented by Propionibacterium freudenreichii: a new vector to study probiotic potentialities in vivo. *Food Microbiol* 2012;**32**:135–46. https://doi.org/10.1016/j.fm.2012.05.003.

da Luz BSR, de Rezende Rodovalho V, Nicolas A *et al.* Impact of environmental conditions on the protein content of *Staphylococcus* aureus and its derived extracellular vesicles. *Microorganisms* 2022;**10**:1808. https://doi.org/10.3390/microorganisms10091808.

Dagnelie M, Corvec S, Khammari A *et al.* Bacterial extracellular vesicles: a new way to decipher host-microbiota communications in inflammatory dermatoses. *Exp Dermatol* 2020;**29**:22–28. https://doi.org/10.1111/exd.14050.

Dauros Singorenko P, Chang V, Whitcombe A *et al.* Isolation of membrane vesicles from prokaryotes: a technical and biological comparison reveals heterogeneity. *J Extracell Vesicles* 2017;**6**:324731. https://doi.org/10.1080/20013078.2017.1324731.

Deatherage BL, Cookson BT. Membrane vesicle release in bacteria, Eukaryotes, and Archaea: a conserved yet underappreciated aspect of microbial life. *Infect Immun* 2012;**80**:1948–57. https://doi.org/10.1128/IAI.06014-11.

Dell'Annunziata F, Folliero V, Giugliano R *et al.* Gene transfer potential of outer membrane vesicles of Gram-negative Bacteria. *Int J Mol Sci* 2021;**22**:5985. https://doi.org/10.3390/ijms22115985.

Deutsch S-MM, Mariadassou M, Nicolas P *et al.* Identification of proteins involved in the anti-inflammatory properties of *Propionibacterium freudenreichii* by means of a multi-strain study. *Sci Rep*. 2017;**7**:46409. https://doi.org/10.1038/srep46409.

do Carmo FLR, Rabah H, Cordeiro BF *et al.* Probiotic *Propionibacterium freudenreichii* requires SlpB protein to mitigate mucositis induced by chemotherapy. *Oncotarget* 2019;**10**:7198–219. https://doi.org/10.18632/oncotarget.27319.

do Carmo FLR, Rabah H, Huang S *et al. Propionibacterium freudenreichii* surface protein SlpB is involved in adhesion to intestinal HT-29 cells. *Front Microbiol* 2017;**8**:1–11. https://doi.org/10.3389/fmicb.2017.01033.

dos Reis M. Unexpected correlations between gene expression and codon usage bias from microarray data for the whole Escherichia coli K-12 genome. *Nucleic Acids Res*. 2003;**31**:6976–85. https://doi.org/10.1093/nar/gkg897.

Elhenawy W, Debelyy MO, Feldman MF. Preferential packing of acidic glycosidases and proteases into bacteroides outer membrane vesicles. *mBio* 2014;**5**:e00909. https://doi.org/10.1128/mBio.00909-14.

Fábrega M-J, Rodríguez-Nogales A, Garrido-Mesa J *et al.* Intestinal anti-inflammatory effects of outer membrane vesicles from *Escherichia coli* Nissle 1917 in DSS-experimental colitis in mice. *Front Microbiol* 2017;**8**:1274. https://doi.org/10.3389/fmicb.2017.01274.

Flemming H-C, Wingender J, Szewzyk U *et al.* Biofilms: an emergent form of bacterial life. *Nat Rev Microbiol* 2016;**14**:563–75. https://doi.org/10.1038/nrmicro.2016.94.

Folador EL, Hassan SS, Lemke N *et al.* An improved interolog mapping-based computational prediction of protein-protein interactions with increased network coverage. *Integr Biol* 2014;**6**:1080–7. https://doi.org/10.1039/c4ib00136b.

Gagnaire V, Jardin J, Rabah H *et al.* Emmental cheese environment enhances *Propionibacterium freudenreichii* stress tolerance. *PLoS One* 2015;**10**:e0135780. https://doi.org/10.1371/journal.pone.0135780.

Gan Y, Li C, Peng X *et al.* Fight bacteria with bacteria: bacterial membrane vesicles as vaccines and delivery nanocarriers against bacterial infections. *Nanomed Nanotechnol Biol Med* 2021;**35**:102398. https://doi.org/10.1016/j.nano.2021.102398.

Gaucher F, Bonnassie S, Rabah H *et al.* Data from a proteomic analysis highlight different osmoadaptations in two strain of Propionibacterium freudenreichii. *Data Br* 2020a;**28**,104932. https://doi.org/10.1016/j.dib.2019.104932.

Gaucher F, Rabah H, Kponouglo K *et al.* Intracellular osmoprotectant concentrations determine *Propionibacterium freudenreichii* survival during drying. *Appl Microbiol Biotechnol* 2020b;**104**:3145–56. https://doi.org/10.1007/s00253-020-10425-1.

Gho YS, Lee C. Emergent properties of extracellular vesicles: a holistic approach to decode the complexity of intercellular communication networks. *Mol Biosyst* 2017;**13**:1291–6. https://doi.org/10.1039/c7mb00146k.

Gilmore WJ, Johnston EL, Zavan L *et al.* Immunomodulatory roles and novel applications of bacterial membrane vesicles. *Mol Immunol* 2021;**134**:72–85. https://doi.org/10.1016/j.molimm.2021.02.027.

Godlewska R, Klim J, Debski J *et al.* Influence of environmental and genetic factors on proteomic profiling of outer membrane vesicles from campylobacter jejuni. *Polish J Microbiol* 2019;**68**:255–61. https://doi.org/10.33073/PJM-2019-027.

Granato D, Bergonzelli GE, Pridmore RD *et al.* Cell surface-associated elongation factor tu mediates the attachment of *Lactobacillus johnsonii* NCC533 (La1) to human intestinal cells and mucins. *Infect Immun* 2004;**72**:2160–9. https://doi.org/10.1128/IAI.72.4.2160-2169.2004.

Gul L, Modos D, Fonseca S *et al.* Extracellular vesicles produced by the human commensal gut bacterium *Bacteroides thetaiotaomicron* affect host immune pathways in a cell-type specific manner that are altered in inflammatory bowel disease. *J Extracell Vesicle* 2022;**11**:e12189. https://doi.org/10.1002/jev2.12189.

Hao H, Zhang X, Tong L *et al.* Effect of extracellular vesicles derived from *Lactobacillus plantarum* Q7 on gut microbiota and ulcerative colitis in mice. *Front Immunol* 2021;**12**:12. https://doi.org/10.3389/fimmu.2021.777147.

He X, Yuan F, Lu F *et al.* Vancomycin-induced biofilm formation by methicillin-resistant *Staphylococcus aureus* is associated with the secretion of membrane vesicles. *Microb Pathog* 2017;**110**:225–31. https://doi.org/10.1016/j.micpath.2017.07.004.

Holay M, Guo Z, Pihl J *et al.* Bacteria-inspired nanomedicine. *ACS Appl Bio Mater* 2021;**4**:3830–48. https://doi.org/10.1021/acsabm.0c01072.

Hong J, Dauros-Singorenko P, Whitcombe A *et al.* Analysis of the *Escherichia coli* extracellular vesicle proteome identifies markers of purity and culture conditions. *J Extracell Vesicles* 2019;**8**:1632099. https://doi.org/10.1080/20013078.2019.1632099.

Huang S, Rabah H, Jardin J *et al.* Hyperconcentrated sweet whey, a new culture medium that enhances *Propionibacterium freudenre-*

ichii stress tolerance. *Appl Environ Microbiol* 2016;**82**:4641–51. https://doi.org/10.1128/AEM.00748-16.

Huerta-Cepas J, Forslund K, Coelho LP *et al.* Fast genome-wide functional annotation through orthology assignment by eggNOG-mapper. *Mol Biol Evol* 2017;**34**:2115–22. https://doi.org/10.1093/molbev/msx148.

Huerta-Cepas J, Szklarczyk D, Heller D *et al.* EggNOG 5.0: a hierarchical, functionally and phylogenetically annotated orthology resource based on 5090 organisms and 2502 viruses. *Nucleic Acids Res* 2019;**47**:D309–14. https://doi.org/10.1093/nar/gky1085.

Jahromi LP, Fuhrmann G. Bacterial extracellular vesicles: understanding biology promotes applications as nanopharmaceuticals. *Adv Drug Deliv Rev* 2021;**173**:125–40. https://doi.org/10.1016/j.addr.2021.03.012.

Jiang L, Schinkel M, van Essen M *et al.* Bacterial membrane vesicles as promising vaccine candidates. *Eur J Pharm Biopharm* 2019;**145**:1–6. https://doi.org/10.1016/j.ejpb.2019.09.021.

Joshi B, Singh B, Nadeem A *et al.* Transcriptome profiling of *Staphylococcus aureus* associated extracellular vesicles reveals presence of small RNA-Cargo. *Front Mol Biosci* 2021;**7**:566207. https://doi.org/10.3389/fmolb.2020.566207.

Keshavarz Azizi Raftar S, Ashrafian F, Yadegar A *et al.* The protective effects of live and pasteurized *Akkermansia muciniphila* and its extracellular vesicles against HFD/CCl4-induced liver injury. *Microbiol Spectr*. 2021;**9**:e0048421. https://doi.org/10.1128/Spectrum.00484-21.

Kesimer M, Kiliç N, Mehrotra R *et al.* Identification of salivary mucin MUC7 binding proteins from *Streptococcus gordonii*. *BMC Microbiol* 2009;**9**:163. https://doi.org/10.1186/1471-2180-9-163.

Kim DJ, Yang J, Seo H *et al.* Colorectal cancer diagnostic model utilizing metagenomic and metabolomic data of stool microbial extracellular vesicles. *Sci Rep* 2020a;**10**:1–10. https://doi.org/10.1038/s41598-020-59529-8.

Kim H, Kim M, Myoung K *et al.* Comparative lipidomic analysis of extracellular vesicles derived from *Lactobacillus plantarum* APsulloc 331261 living in green tea leaves using liquid chromatography-mass spectrometry. *Int J Mol Sci* 2020b;**21**:8076. https://doi.org/10.3390/ijms21218076.

Kim JH, Lee J, Park J *et al.* Gram-negative and Gram-positive bacterial extracellular vesicles. *Semin Cell Dev Biol* 2015;**40**:97–104. https://doi.org/10.1016/j.semcdb.2015.02.006.

Klimentová J, Stulík J. Methods of isolation and purification of outer membrane vesicles from gram-negative bacteria. *Microbiol Res* 2015;**170**:1–9. https://doi.org/10.1016/j.micres.2014.09.006.

Kugeratski FG, Hodge K, Lilla S *et al.* Quantitative proteomics identifies the core proteome of exosomes with syntenin-1 as the highest abundant protein and a putative universal biomarker. *Nat Cell Biol* 2021;**23**:631–41. https://doi.org/10.1038/s41556-021-00693-y.

Laemmli UK. Cleavage of structural proteins during the assembly of the head of bacteriophage T4. *Nature* 1970;**227**:680–5. https://doi.org/10.1038/227680a0.

Langella O, Valot B, Balliau T *et al.* X!TandemPipeline: a tool to manage sequence redundancy for protein inference and phosphosite identification. *J Proteome Res* 2017;**16**:494–503. https://doi.org/10.1021/acs.jproteome.6b00632.

Lee BD. Python implementation of codon adaptation index. *J Open Source Softw* 2018;**3**:905. https://doi.org/10.21105/joss.00905.

Lee EY, Choi DY, Kim DK *et al.* Gram-positive bacteria produce membrane vesicles: proteomics-based characterization of *Staphylococcus aureus*-derived membrane vesicles. *Proteomics* 2009;**9**:5425–36. https://doi.org/10.1002/pmic.200900338.

Lee J, Lee EY, Kim SH *et al.* *Staphylococcus aureus* extracellular vesicles carry biologically active β-lactamase. *Antimicrob Agents Chemother* 2013;**57**:2589–95. https://doi.org/10.1128/AAC.00522-12.

Lemaître G, Nogueira F, Aridas CK. Imbalanced-learn: a python toolbox to tackle the curse of imbalanced datasets in machine learning. *J Mach Learn Res* 2017;**18**:1–5. http://jmlr.org/papers/v18/16-365.html.

Li Y, Ma X, Yue Y *et al.* Rapid surface display of mRNA antigens by bacteria-derived outer membrane vesicles for a personalized tumor vaccine. *Adv Mater* 2022;**34**:2109984. https://doi.org/10.1002/adma.202109984.

Li Z, Clarke AJ, Beveridge TJ. Gram-negative bacteria produce membrane vesicles which are capable of killing other bacteria. *J Bacteriol* 1998;**180**:5478–83. https://doi.org/10.1128/JB.180.20.5478-5483.1998.

Liu Y, Alexeeva S, Defourny KA *et al.* Tiny but mighty: bacterial membrane vesicles in food biotechnological applications. *Curr Opin Biotechnol* 2018;**49**:179–84. https://doi.org/10.1016/j.copbio.2017.09.001.

López P, González-Rodríguez I, Sánchez B *et al.* Treg-inducing membrane vesicles from Bifidobacterium bifidum LMG13195 as potential adjuvants in immunotherapy. *Vaccine* 2012;**30**:825–9. https://doi.org/10.1016/j.vaccine.2011.11.115.

Lundberg SM, Erion G, Chen H *et al.* From local explanations to global understanding with explainable AI for trees. *Nat Mach Intell* 2020;**2**:56–67.

Lundberg SM, Lee S-I. "A unified approach to interpreting model predictions," In: Guyon I, Luxburg UV, Bengio S, Wallach H, Fergus R, Vishwanathan S (eds.), *Advances in Neural Information Processing Systems*. **Vol. 30**, New York: Curran Associates, Inc, 2017, 4765–74.

Luz B, Nicolas A, Chabelskaya S *et al.* Environmental plasticity of the RNA content of *Staphylococcus aureus* extracellular vesicles. *Front Microbiol* 2021;**12**:12. https://doi.org/10.3389/fmicb.2021.634226.

Lynch JB, Schwartzman JA, Bennett BD *et al.* Ambient pH alters the protein content of outer membrane vesicles, driving host development in a beneficial symbiosis. *J Bacteriol* 2019;**201**. https://doi.org/10.1128/JB.00319-19.

Macek B, Forchhammer K, Hardouin J *et al.* Protein post-translational modifications in bacteria. *Nat Rev Microbiol* 2019;**17**:651–64. https://doi.org/10.1038/s41579-019-0243-0.

Malik AC, Reinbold GW, Vedamuthu ER. An evaluation of the taxonomy of Propionibacterium. *Can J Microbiol* 1968;**14**:1185–91. https://doi.org/10.1139/m68-199.

Manning AJ, Kuehn MJ. Contribution of bacterial outer membrane vesicles to innate bacterial defense. *BMC Microbiol* 2011;**11**:258. https://doi.org/10.1186/1471-2180-11-258.

Mashburn LM, Whiteley M. Membrane vesicles traffic signals and facilitate group activities in a prokaryote. *Nature* 2005;**437**:422–5. https://doi.org/10.1038/nature03925.

McKinney W. Data structures for statistical computing in python. in proceedings of the 9th python in science conference. 2010;56–61. https://doi.org/10.25080/Majora-92bf1922-00a.

McNamara RP, Dittmer DP. Modern techniques for the isolation of extracellular vesicles and viruses. *J Neuroimmune Pharmacol* 2020;**15**:459–72. https://doi.org/10.1007/s11481-019-09874-x.

Mehanny M, Kroniger T, Koch M *et al.* Yields and immunomodulatory effects of pneumococcal membrane vesicles differ with the bacterial growth phase. *Adv Healthc Mater* 2022;**11**:2101151. https://doi.org/10.1002/adhm.202101151.

Merico D, Isserlin R, Stueker O *et al.* Enrichment map: a network-based method for gene-set enrichment visualization and interpretation. *PLoS One* 2010;**5**:e13984. https://doi.org/10.1371/journal.pone.0013984.

Mirjafari Tafti ZS, Moshiri A, Ettehad Marvasti F *et al.* The effect of saturated and unsaturated fatty acids on the production of outer membrane vesicles from *Bacteroides fragilis* and *Bacteroides thetaiotaomicron*. *Gastroenterol Hepatol from Bed to Bench* 2019;**12**:155–62. Available at: http://www.ncbi.nlm.nih.gov/pubmed/31191841.

Mol EA, Goumans MJ, Doevendans PA *et al.* Higher functionality of extracellular vesicles isolated using size-exclusion chromatography compared to ultracentrifugation. *Nanomed Nanotechnol Biol Med* 2017;**13**:2061–5. https://doi.org/10.1016/j.nano.2017.03.011.

Molina-Tijeras JA, Gálvez J, Rodríguez-Cabezas ME *et al.* The immunomodulatory properties of extracellular vesicles derived from probiotics: a novel approach for the management of gastrointestinal diseases. *Nutrients* 2019;**11**:1038. https://doi.org/10.3390/nu11051038.

Monguió-Tortajada M, Gálvez-Montón C, Bayes-Genis A *et al.* Extracellular vesicle isolation methods: rising impact of size-exclusion chromatography. *Cell Mol Life Sci*, 2019;**76**:2369–82. https://doi.org/10.1007/s00018-019-03071-y.

Monteiro R, Chafsey I, Ageorges V *et al.* The secretome landscape of *Escherichia coli* O157:H7: deciphering the cell-surface, outer membrane vesicle and extracellular subproteomes. *J Proteomics* 2021;**232**:104025. https://doi.org/10.1016/j.jprot.2020.104025.

Nagakubo T, Nomura N, Toyofuku M. Cracking open bacterial membrane vesicles. *Front Microbiol* 2020;**10**:3026. https://doi.org/10.3389/fmicb.2019.03026.

Nishiyama K, Takaki T, Sugiyama M *et al.* Extracellular vesicles produced by Bifidobacterium longum export mucin-binding proteins. *Appl Environ Microbiol* 2020;**86**:1–11. https://doi.org/10.1128/AEM.01464-20.

Nordin JZ, Lee Y, Vader P *et al.* Ultrafiltration with size-exclusion liquid chromatography for high yield isolation of extracellular vesicles preserving intact biophysical and functional properties. *Nanomed Nanotechnol Biol Med* 2015;**11**:879–83. https://doi.org/10.1016/j.nano.2015.01.003.

Park J, Kim N-E, Yoon H *et al.* Fecal microbiota and gut microbe-derived extracellular vesicles in colorectal cancer. *Front Oncol* 2021;**11**:11. https://doi.org/10.3389/fonc.2021.650026.

Pathirana RD, Kaparakis-Liaskos M. Bacterial membrane vesicles: biogenesis, immune regulation and pathogenesis. *Cell Microbiol* 2016;**18**:1518–24. https://doi.org/10.1111/cmi.12658.

Pedregosa F, Varoquaux G, Gramfort A *et al.* Scikit-learn: machine learning in python. *J Mach Learn Res* 2011;**12**:2825–30. http://jmlr.org/papers/v12/pedregosa11a.html.

Pérez-Cruz C, Briansó F, Sonnleitner E *et al.* RNA release *via* membrane vesicles in *Pseudomonas aeruginosa* PAO1 is associated with the growth phase. *Environ Microbiol* 2021;**23**:5030–41. https://doi.org/10.1111/1462-2920.15436.

Potter M, Hanson C, Anderson AJ *et al.* Abiotic stressors impact outer membrane vesicle composition in a beneficial rhizobacterium: Raman spectroscopy characterization. *Sci Rep* 2020;**10**:21289. https://doi.org/10.1038/s41598-020-78357-4.

Prados-Rosales R, Weinrick BC, Piqué DG *et al.* Role for mycobacterium tuberculosis membrane vesicles in iron acquisition. *J Bacteriol* 2014;**196**:1250–6. https://doi.org/10.1128/JB.01090-13.

Rakoff-Nahoum S, Coyne MJ, Comstock LE. An ecological network of polysaccharide utilization among human intestinal symbionts. *Curr Biol* 2014;**24**:40–49. https://doi.org/10.1016/j.cub.2013.10.077.

Raudvere U, Kolberg L, Kuzmin I *et al.* G:profiler: a web server for functional enrichment analysis and conversions of gene lists (2019 update). *Nucleic Acids Res* 2019;**47**:W191–8. https://doi.org/10.1093/nar/gkz369.

Reimand J, Isserlin R, Voisin V *et al.* Pathway enrichment analysis and visualization of omics data using g:profiler, GSEA, Cytoscape and EnrichmentMap. *Nat Protoc* 2019;**14**:482–517. https://doi.org/10.1038/s41596-018-0103-9.

Rodovalho V, de R, da Luz BSR *et al.* Environmental conditions modulate the protein content and immunomodulatory activity of extracellular vesicles produced by the probiotic *Propionibacterium freudenreichii*. *Appl Environ Microbiol* 2021;**87**:1–16. https://doi.org/10.1128/AEM.02263-20.

Rodovalho VdR, Luz BSRd, Rabah H *et al.* Extracellular vesicles produced by the probiotic *Propionibacterium freudenreichii* CIRM-BIA 129 mitigate inflammation by modulating the NF-κB pathway. *Front Microbiol* 2020;**11**:1544. https://doi.org/10.3389/fmicb.2020.01544.

Rubio APD, Martínez JH, Casillas DCM *et al.* Lactobacillus casei BL23 produces microvesicles carrying proteins that have been associated with its probiotic effect. *Front Microbiol* 2017;**8**:1–12. https://doi.org/10.3389/fmicb.2017.01783.

Sarshar M, Scribano D, Ambrosi C *et al.* Fecal microRNAs as innovative biomarkers of intestinal diseases and effective players in host-microbiome interactions. *Cancers (Basel)*. 2020;**12**:2174. https://doi.org/10.3390/cancers12082174.

Sartorio MG, Valguarnera E, Hsu F-F *et al.* Lipidomics analysis of outer membrane vesicles and elucidation of the inositol phosphoceramide biosynthetic pathway in bacteroides thetaiotaomicron. *Microbiol Spectr* 2022;**10**:1–13. https://doi.org/10.1128/spectrum.00634-21.

Schlatterer K, Beck C, Hanzelmann D *et al.* The mechanism behind bacterial lipoprotein release: phenol-soluble modulins mediate toll-like receptor 2 activation via extracellular vesicle release from *Staphylococcus aureus*. *mBio* 2018;**9**:e01851–18. https://doi.org/10.1128/mBio.01851-18.

Schou AS, Nielsen JE, Askeland A *et al.* Extracellular vesicle-associated proteins as potential biomarkers. *Adv Clin Chem* 2020;**99**:1–48. https://doi.org/10.1016/bs.acc.2020.02.011.

Seo MKK, Park EJJ, Ko SYY *et al.* Therapeutic effects of kefir grain *Lactobacillus*-derived extracellular vesicles in mice with 2,4,6-trinitrobenzene sulfonic acid-induced inflammatory bowel disease. *J Dairy Sci* 2018;**101**:8662–71. https://doi.org/10.3168/jds.2018-15014.

Shannon P, Markiel A, Ozier O *et al.* Cytoscape: a software environment for integrated models of biomolecular interaction networks. *Genome Res* 2003;**13**:2498–504. https://doi.org/10.1101/gr.1239303.

Sharp PM, Li W-H. The codon adaptation index-a measure of directional synonymous codon usage bias, and its potential applications. *Nucl Acids Res* 1987;**15**:1281–95. https://doi.org/10.1093/nar/15.3.1281.

Shen Y, Torchia MLG, Lawson GW *et al.* Outer membrane vesicles of a human commensal mediate immune regulation and disease protection. *Cell Host Microbe* 2012;**12**:509–20. https://doi.org/10.1016/j.chom.2012.08.004.

Switzer RC, Merril CR, Shifrin S. A highly sensitive silver stain for detecting proteins and peptides in polyacrylamide gels. *Anal Biochem* 1979;**98**:231–7. https://doi.org/10.1016/0003-2697(79)90732-2.

Szklarczyk D, Gable AL, Nastou KC *et al.* The STRING database in 2021: customizable protein–protein networks, and functional characterization of user-uploaded gene/measurement sets. *Nucleic Acids Res.* 2021;**49**:D605–12. https://doi.org/10.1093/nar/gkaa1074.

Tartaglia NR, Breyne K, Meyer E *et al.* *Staphylococcus aureus* extracellular vesicles elicit an immunostimulatory response in vivo on

the murine mammary gland. *Front Cell Infect Microbiol* 2018;**8**:277. https://doi.org/10.3389/fcimb.2018.00277.

Tartaglia NR, Nicolas A, Rodovalho VdR *et al.* Extracellular vesicles produced by human and animal *Staphylococcus aureus* strains share a highly conserved core proteome. *Sci Rep* 2020;**10**:8467. https://doi.org/10.1038/s41598-020-64952-y.

The Pandas Development Team. pandas-dev/pandas: Pandas (v2.0.2). Zenodo. 2020. https://doi.org/10.5281/zenodo.7979740.

Toyofuku M, Cárcamo-Oyarce G, Yamamoto T *et al.* Prophage-triggered membrane vesicle formation through peptidoglycan damage in Bacillus subtilis. *Nat Commun* 2017;**8**:1–10. https://doi.org/10.1038/s41467-017-00492-w.

Urabe F, Kosaka N, Ito K *et al.* Extracellular vesicles as biomarkers and therapeutic targets for cancer. *Am J Physiol-Cell Physiol* 2020;**318**:C29–39. https://doi.org/10.1152/ajpcell.00280.2019.

Useckaite Z, Rodrigues AD, Hopkins AM *et al.* Role of extracellular vesicle-derived biomarkers in drug metabolism and disposition. *Drug Metab Dispos* 2021;**49**:961–71. https://doi.org/10.1124/dmd.121.000411.

Valguarnera E, Scott NE, Azimzadeh P *et al.* Surface exposure and packing of lipoproteins into outer membrane vesicles are coupled processes in bacteroides. *mSphere* 2018;**3**:e00559–18. https://doi.org/10.1128/mSphere.00559-18.

Vargoorani ME, Modarressi MH, Vaziri F *et al.* Stimulatory effects of *Lactobacillus* casei derived extracellular vesicles on toll-like receptor 9 gene expression and cytokine profile in human intestinal epithelial cells. *J Diabetes Metab Disord* 2020;**19**:223–31. https://doi.org/10.1007/s40200-020-00495-3.

Vestad B, Llorente A, Neurauter A *et al.* Size and concentration analyses of extracellular vesicles by nanoparticle tracking analysis: a variation study. *J Extracell Vesicles* 2017;**6**: 1344087. https://doi.org/10.1080/20013078.2017.1344087.

Waskom M, Botvinnik O, O'Kane D *et al.* 2017. mwaskom/seaborn: v0.8.1 September 2017. Zenodo. https://doi.org/10.5281/zenodo.883859.

Wickham H 2016. *ggplot2: Elegant Graphics for Data Analysis*. New York: Springer. https://ggplot2.tidyverse.org.

Woith E, Fuhrmann G, Melzig MF. Extracellular Vesicles—Connecting Kingdoms. *Int J Mol Sci* 2019;**20**:5695. https://doi.org/10.3390/ijms20225695.

Xu P, Baldridge RD, Chi RJ *et al.* Phosphatidylserine flipping enhances membrane curvature and negative charge required for vesicular transport. *J Cell Biol* 2013;**202**:875–86. https://doi.org/10.1083/jcb.201305094.

Yang J, Kim EK, McDowell A *et al.* Microbe-derived extracellular vesicles as a smart drug delivery system. *Transl Clin Pharmacol* 2018;**26**:103. https://doi.org/10.12793/tcp.2018.26.3.103.

Yu CS, Cheng CW, Su WC *et al.* CELLO2GO: a web server for protein subCELlular lOcalization prediction with functional gene ontology annotation. *PLoS One* 2014;**9**:e99368. https://doi.org/10.1371/journal.pone.0099368.

Yun SH, Park EC, Lee S-Y *et al.* Antibiotic treatment modulates protein components of cytotoxic outer membrane vesicles of multidrug-resistant clinical strain, *Acinetobacter baumannii* DU202.*Clin Proteom* 2018;**15**:28. https://doi.org/10.1186/s12014-018-9204-2.

Zhuang Q, Xu J, Deng D *et al.* Bacteria-derived membrane vesicles to advance targeted photothermal tumor ablation. *Biomaterials* 2021;**268**:120550. https://doi.org/10.1016/j.biomaterials.2020.120550.

Zwarycz AS, Livingstone PG, Whitworth DE. Within-species variation in OMV cargo proteins: the *Myxococcus xanthus* OMV panproteome. *Mol Omics* 2020;**16**:387–97. https://doi.org/10.1039/D0MO00027B.

Received 15 December 2022; **revised** 12 May 2023; **accepted** 31 May 2023